








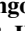



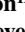








The Complex Exhumation History of Jezero Crater Floor Unit and Its Implication for Mars Sample Return

Special Section:

The Mars Perseverance Rover
Jezero Crater Floor Campaign

C. Quantin-Nataf¹ , S. Alwmark^{2,3} , F. J. Calef⁴ , J. Lasue⁵ , K. Kinch⁶ , K. M. Stack⁴, V. Sun⁴ ,
N. R. Williams⁴ , E. Dehouck¹ , L. Mandon⁷ , N. Mangold⁸ , O. Beyssac⁹ , E. Clave¹⁰ ,
S. H. G. Walter¹¹ , J. I. Simon¹² , A. M. Annex^{13,14} , B. Horgan¹⁵ , James W. Rice Jr.¹⁶, D. Shuster¹⁷,
B. Cohen¹⁸ , L. Kah¹⁹ , Steven Sholes⁴ , and B. P. Weiss^{4,20} 

Key Points:

- The dark floor unit of the Jezero crater displays an unusual inhomogeneous crater density, suggesting a complex exhumation history
- The crater density of the dark crater floor unit corresponds to the exposure time post exhumation
- The crater density of this unit will not allow the calibration of the Martian crater chronology from return samples

Correspondence to:

C. Quantin-Nataf,
cathy.quantin@univ-lyon1.fr

Citation:

Quantin-Nataf, C., Alwmark, S., Calef, F. J., Lasue, J., Kinch, K., Stack, K. M., et al. (2023). The complex exhumation history of Jezero crater floor unit and its implication for Mars sample return. *Journal of Geophysical Research: Planets*, 128, e2022JE007628. <https://doi.org/10.1029/2022JE007628>

Received 19 OCT 2022
Accepted 17 MAY 2023

Author Contributions:

Conceptualization: C. Quantin-Nataf, S. Alwmark, J. Lasue, J. I. Simon, D. Shuster
Data curation: C. Quantin-Nataf, F. J. Calef, N. R. Williams
Formal analysis: C. Quantin-Nataf, F. J. Calef, J. Lasue, V. Sun, N. Mangold, S. H. G. Walter, A. M. Annex, D. Shuster
Funding acquisition: C. Quantin-Nataf
Investigation: C. Quantin-Nataf, S. Alwmark, F. J. Calef, K. Kinch, K. M. Stack, V. Sun, E. Dehouck, L. Mandon, N. Mangold, O. Beyssac, E. Clave, J. I. Simon, B. Cohen, L. Kah, Steven Sholes, B. P. Weiss
Methodology: C. Quantin-Nataf, S. Alwmark, J. Lasue, E. Dehouck, L. Mandon, B. Horgan, James W. Rice Jr., D. Shuster
Project Administration: C. Quantin-Nataf

¹Laboratoire de Géologie de Lyon: Terre, Planètes, Environnement, Université de Lyon, Université Claude Bernard Lyon1, Ecole Normale Supérieure de Lyon, Université Jean Monnet Saint Etienne, CNRS, Villeurbanne, France, ²Department of Geology, Lund University, Lund, Sweden, ³Niels Bohr Institute, University of Copenhagen, Copenhagen, Denmark, ⁴Jet Propulsion Laboratory, California Institute of Technology, Pasadena, CA, USA, ⁵Institut de Recherche en Astrophysique et Planétologie, Université de Toulouse 3 Paul Sabatier, Centre National de la Recherche Scientifique, Centre National d'Etude Spatiale, Toulouse, France, ⁶Niels Bohr Institute, University of Copenhagen, Copenhagen, Denmark, ⁷LESIA, Observatoire de Paris, Université PSL, CNRS, Sorbonne Université, Université de Paris, Meudon, France, ⁸Laboratoire Planétologie et Géosciences, CNRS, Nantes Université, Université Angers, Le Mans Université, Nantes, France, ⁹Institut de Minéralogie, de Physique des Matériaux et de Cosmochimie, CNRS, Sorbonne Université, Muséum National d'Histoire Naturelle, Paris, France, ¹⁰Centre Lasers Intenses et Applications, CNRS, CEA, Université de Bordeaux, Bordeaux, France, ¹¹Department of Earth Sciences, Freie Universität Berlin, Institute of Geological Sciences, Planetary Sciences and Remote Sensing Working Group, Berlin, Germany, ¹²Center for Isotope Cosmochemistry and Geochronology, NASA Johnson Space Center, Astromaterials Research and Exploration Science, Houston, TX, USA, ¹³Division of Geological and Planetary Sciences, California Institute of Technology, Pasadena, CA, USA, ¹⁴Morton K. Blaustein Department of Earth & Planetary Sciences, Johns Hopkins University, Baltimore, MD, USA, ¹⁵Department of Earth, Atmospheric, and Planetary Sciences, Purdue University, West Lafayette, IN, USA, ¹⁶School of Earth and Space Exploration, Arizona State University, Tempe, AZ, USA, ¹⁷Department of Earth and Planetary Science, University of California, Berkeley, CA, USA, ¹⁸NASA Goddard Space Flight Center, Greenbelt, MD, USA, ¹⁹Department of Earth and Planetary Sciences, University of Tennessee, Knoxville, TN, USA, ²⁰Department of Earth, Atmospheric and Planetary Sciences, Massachusetts Institute of Technology, Cambridge, MA, USA

Abstract During the first year of NASA's Mars 2020 mission, Perseverance rover has investigated the dark crater floor unit of Jezero crater and four samples of this unit have been collected. The focus of this paper is to assess the potential of these samples to calibrate the crater-based Martian chronology. We first review the previous estimation of crater-based model age of this unit. Then, we investigate the impact crater density distribution across the floor unit. It reveals that the crater density is heterogeneous from areas which have been exposed to the bombardment during the last 3 Ga to areas very recently exposed to bombardment. It suggests a complex history of exposure to impact cratering. We also display evidence of several remnants of deposits on the top of the dark floor unit across Jezero below which the dark floor unit may have been buried. We propose the following scenario of burying/exhumation: the dark floor unit would have been initially buried below a unit that was a few tens of meters thick. This unit then gradually eroded away due to Aeolian processes from the northeast to the west, resulting in uneven exposure to impact bombardment over 3 Ga. A cratering model reproducing this scenario confirms the feasibility of this hypothesis. Due to the complexity of its exposure history, the Jezero dark crater floor unit will require additional detailed analysis to understand how the Mars 2020 mission samples of the crater floor can be used to inform the Martian cratering chronology.

Plain Language Summary Perseverance rover landed within Jezero crater (Mars) in 2021 and is collecting rocks that will be returned to Earth. In terrestrial state-of-the-art labs, these rocks will be dated. It will allow to test the method planetary scientists are using to assess the age of Martian surfaces: their impact crater statistics. As impact craters are forming regularly, their statistics are used as a timeline in planetary sciences. The present paper studies the statistic of impacts craters within Jezero crater to reveal that the floor of Jezero has been protected from bombardment during years. These results imply that the collected rocks of the Jezero crater floor will not be ideal to test the method of using impact crater as chronometer of Martian surfaces.

Resources: C. Quantin-Nataf, F. J. Calef, N. R. Williams, B. Horgan

Software: C. Quantin-Nataf

Supervision: C. Quantin-Nataf, V. Sun, James W. Rice Jr.

Validation: C. Quantin-Nataf, S.

Alwmark, J. Lasue, James W. Rice Jr.

Visualization: C. Quantin-Nataf, F. J. Calef, V. Sun, N. R. Williams, James W. Rice Jr.

Writing – original draft: C. Quantin-Nataf, S. Alwmark, J. Lasue, K. Kinch, E. Dehouck, L. Mandon, N. Mangold, O. Beyssac, E. Clave, S. H. G. Walter, J. I. Simon, A. M. Annex, B. Horgan, James W. Rice Jr., D. Shuster, B. Cohen, L. Kah, Steven Sholes, B. P. Weiss

Writing – review & editing: C. Quantin-Nataf, S. Alwmark, J. Lasue, N. Mangold, O. Beyssac, S. H. G. Walter, J. I. Simon, A. M. Annex, B. Horgan, D. Shuster

1. Introduction

On 18 February 2021, NASA's Mars 2020 Perseverance rover landed on the floor of Jezero crater, a ~50 km-in-diameter crater located at the margin of the Isidis basin. The Mars 2020 mission is the first step of the joint NASA/ESA Mars Sample Return campaign, as the Perseverance rover is collecting and caching rock, regolith, and atmospheric samples for eventual return to Earth. Returning an igneous sample of a crater-retaining surface on Mars is of utmost importance to accomplish the science objectives of Mars sample return (Beaty et al., 2019). It would establish a direct link between a radioisotopic age and a crater density distribution and thus constrain the absolute calibration of the Martian cratering chronology, which is widely used to constrain the timing of geological features and surfaces on Mars.

Several geological units are observed within Jezero crater and these have been extensively studied using orbital data prior to the landing (Brown et al., 2020; Goudge et al., 2015; Stack et al., 2020) (Figure 1): a pyroxene-bearing, cratered dark floor unit; an olivine-bearing, light-toned floor unit exposed in erosional windows below the dark floor unit; a deltaic complex; and a marginal carbonate-bearing unit (B. H. N. Horgan et al., 2020). The dark crater floor unit is relatively flat and cratered, and so would represent a promising sample target for geochronology within Jezero. It was promoted as an asset to select Jezero as a landing site for the Mars 2020 rover.

Yet, the chronology of formation of the Jezero crater floor units has been debated. The leading pre-landing model (e.g., Goudge et al., 2015) for the sequence of events in Jezero crater was (a) the formation of the Isidis impact; (b) the formation of Jezero in the inner margin of Isidis basin; (c) the filling of Jezero crater by the regional olivine bearing unit at about 3.8 Ga (Mandon et al., 2020); (d) the emplacement of the delta and the marginal carbonate-bearing unit during one or more lacustrine phases; and (e) the emplacement of the unaltered mafic floor unit (Goudge et al., 2015). However, high resolution investigation of the stratigraphic relationships between the deltaic deposits and possible distal delta remnants and the dark crater floor unit questions this succession of events (Farley et al., 2022; Holm-Alwmark et al., 2021; Stack et al., 2020). In an alternative model, the deltaic deposits may overlie the floor unit, making the dark floor unit older than Jezero's fluvio-deltaic deposits (Holm-Alwmark et al., 2021). The stratigraphic relationship between the dark cratered floor unit and the delta is not so clear from orbital data analysis. As the crater floor is the only major crater-retaining surface within Jezero, its crater density has been investigated by several independent studies and the ages returned range from 1.4 to 3.5 Ga, that is, from Amazonian to Hesperian (Goudge et al., 2012; Marchi, 2021; Rubanenko et al., 2021; Schon et al., 2012; Shahrzad et al., 2019; Warner et al., 2020). The relatively small areal extent of the unit implies large uncertainties on the age derived from crater statistics (<1,000 km², Warner et al., 2015), but the crater density argues for a floor unit younger than the fluvial activity of Jezero (Goudge et al., 2012; Marchi, 2021; Schon et al., 2012; Shahrzad et al., 2019).

During the first ~380 sols of the mission, the dark crater floor unit, referred to as the Máaz formation by the Mars 2020 team (Farley et al., 2022), has been investigated using the payload on the Perseverance rover. Four samples have been collected from this unit: Montagnac and Montdenier from the Rochette member of the Artuby ridge, a widespread caprock layer within Máaz, and Hahonih and Atsah from the upper crater-retaining top of Maaz (Simon et al., 2023). The results of Perseverance's crater floor scientific campaign (Sun et al., 2022) show that the dark floor unit is composed of holocrystalline igneous rocks dominated by pyroxene and plagioclase with limited aqueous alteration (Farley et al., 2022; Mandon et al., 2022; Udry et al., 2022; Wiens et al., 2022). These rocks have been interpreted as extrusive rocks (Alwmark et al., 2023; B. Horgan et al., 2022; Udry et al., 2022). Their igneous origin and limited alteration make these samples promising for geochronology purposes, if the age of crystallization represents the duration of subsequent crater accumulation.

The purpose of this study is to analyze the quality and relevance of the crater statistics of the Jezero dark crater floor unit to assess if they represent the duration of crater accumulation since the crystallization of the rocks. We will first review the attempts at age estimation of the dark crater floor unit from crater densities, and then investigate the cratering density distribution across the floor unit. We will then discuss the observation of possible sedimentary remnants within Jezero. Finally, using a cratering model, we propose a scenario to reconcile all the observations and discuss its implications.

2. Review of Crater-Based Age Determination of the Dark Crater Floor Unit

Many ancient crater-lakes, including Jezero, host dark toned crater floor units. These are often crater-retaining, pyroxene-rich and non-hydrated, interpreted as volcanic in origin (Goudge et al., 2012), and predominantly post-date the lacustrine activity. As these units are crater-retaining, they are key to constrain the cessation of the lacustrine activity (Goudge et al., 2012). Using the 5 largest craters ($D > 850$ m) observed within Jezero's dark

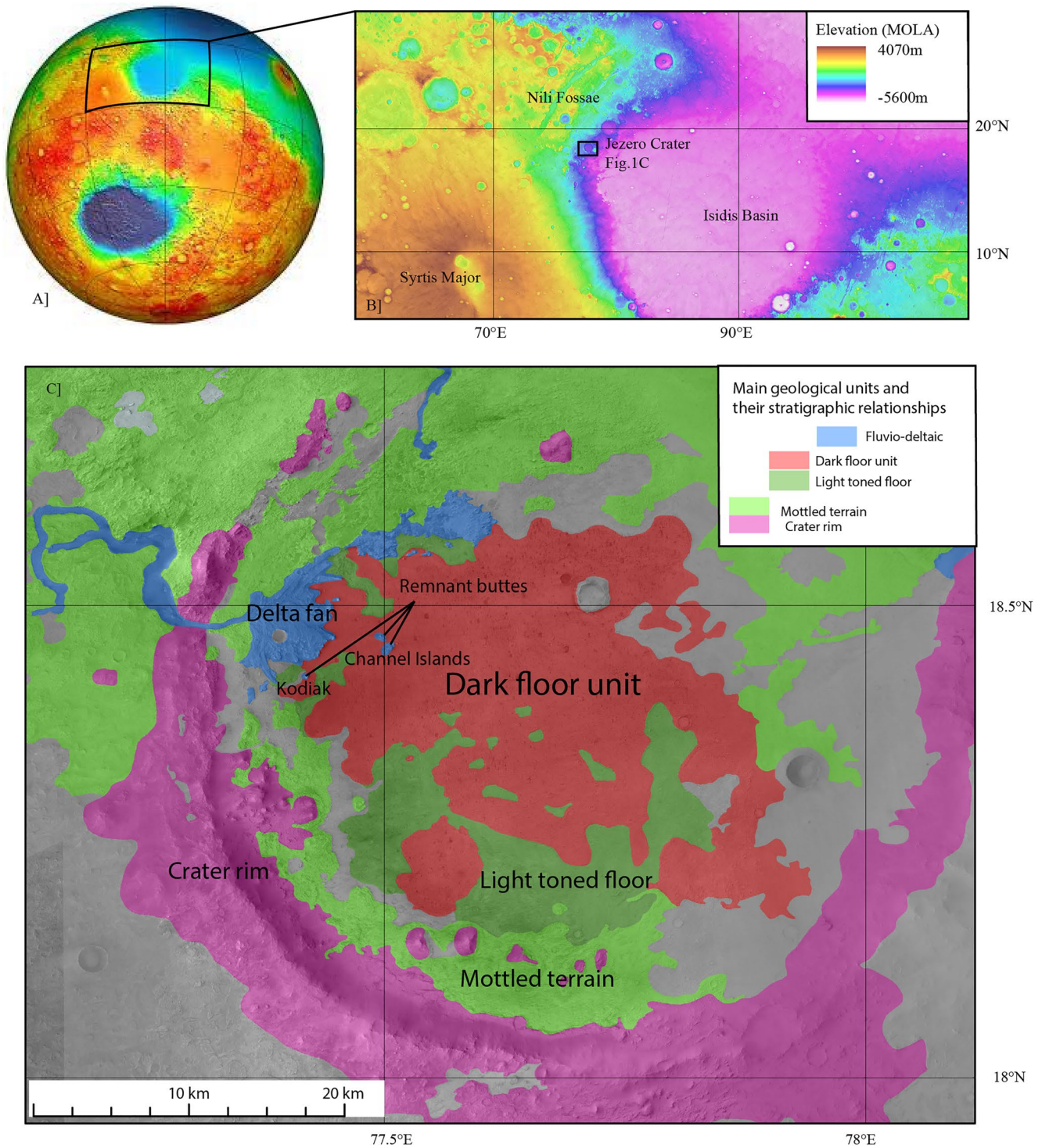


Figure 1. (a) Mola Hemispheric view of Mars with the location of (b). (b) Regional context of (c) MOLA topography is displayed in transparency over Themis Day-time mosaic (Smith et al., 2003). (c) Simplified geological context of the Jezero dark crater floor unit (here in red). The geological unit contours are from Goudge et al. (2015). The interpretation of the remnant deposit is from Stack et al. (2020) and Mangold et al. (2021). The stratigraphic relationships displayed in the legend are from Holm-Alwmark et al. (2021) who argued for a dark floor unit pre-dating the deltaic deposits.

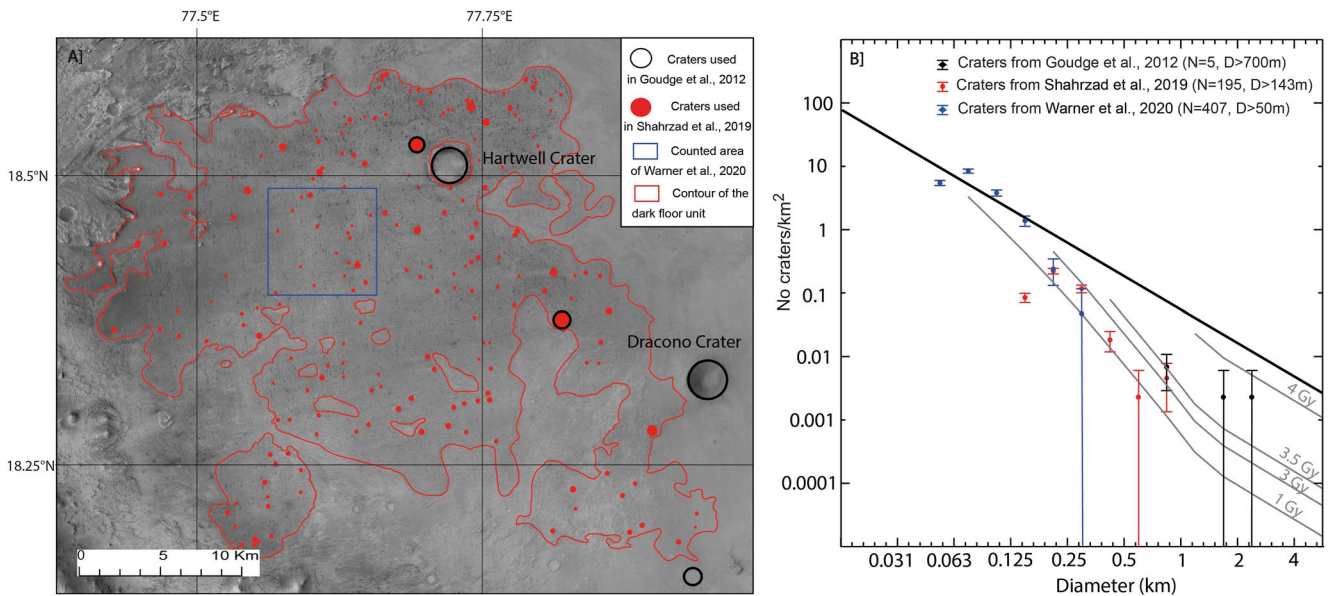


Figure 2. Previous crater-based age determinations of the dark floor unit in Jezero crater. (a) Mosaic of CTX images with the dark floor unit contoured in red. The craters outlined in black are the ones used in Goudge et al. (2012); the craters colored in red are the ones used in Shahrzad et al. (2019) and the blue box is the counted area at High Resolution Imaging Science Experiment scale of Warner et al. (2020). Note that Hartwell crater, despite being located within the dark floor unit, has not been included in the age determination of Shahrzad et al. (2019). (b) Incremental plot of the crater size frequency distributions (Hartmann & Neukum, 2001) of the crater populations used for age determination of the dark floor unit of in Goudge et al. (dark diamonds), Shahrzad et al. (red diamonds) and Warner et al. (blue diamonds), respectively. The bold line is the saturation line (Hartmann & Neukum, 2001) and the gray lines are isochrons: the theoretical crater size frequency distributions of a surface exposed to bombardment without subsequent modification from Hartmann (2005). Note that the overturn observed in the smallest crater diameters of the distribution of both Goudge et al. and Shahrzad et al. is explained by a resolution effect.

floor unit, Goudge et al. estimated its age to 3.45 Ga, thus placing the end of the lacustrine activity near the Noachian-Hesperian transition (Goudge et al., 2012).

Shahrzad et al. dedicated an entire study to the careful mapping of the Jezero dark floor unit and the superimposed craters ($D > 100$ m). The unit is easy to identify and map thanks to its singular color and aspect and thanks to its boundary forming a ~ 20 m thick cliff (Shahrzad et al., 2019). They obtained a model age of $2.6 \text{ Ga} \pm 0.5 \text{ Ga}$ (statistical uncertainty) based on crater size-frequency distribution (CSFD) measurements of craters in the size range $177 \text{ m} < D < 500 \text{ m}$ (Shahrzad et al., 2019). Shahrzad et al. point out that the Goudge et al. age comes with a very large statistical uncertainty because it is based on only 5 craters. Shahrzad et al. argued that the 3 largest craters used by Goudge et al. are not relevant for dating this surface (Shahrzad et al., 2019). Two craters (including Dracono; Figure 2) were excluded because they were not located within the re-mapped dark crater floor unit and the third one (Hartwell) because of its unusual shape suggesting that it may pre-date the emplacement of the floor unit (Shahrzad et al., 2019).

As observed in Figure 2, the size-frequency distribution of the craters used by Shahrzad et al. follows the isochron slope, which corresponds to a theoretical trend of unmodified impact cratering (e.g., Hartmann & Neukum, 2001). In contrast, any deviation from this slope would indicate the modification of the crater population by subsequent processes (e.g., Michael, 2013; Quantin-Nataf et al., 2019). For instance, erosion tends to reduce the population of smaller craters more rapidly than larger craters and leads to a crater size distribution with a slope lower than those of the isochrons (e.g., Kite & Mayer, 2017; Michael, 2013; Quantin-Nataf et al., 2019). This is not the case on the dark floor unit of Jezero, which strongly indicates that the population of craters has not been modified since the unit was first exposed to the meteoritic bombardment. This argument strengthens the young model age found by Shahrzad et al. (2019).

Warner et al. (2020) performed a crater statistical analysis of smaller craters (>50 m) in a subset area located in the center of the dark floor unit and obtained a crater retention age around 2.3 Ga and a CSFD following the slope of the isochrons (Figure 2), confirming the Amazonian age of this unit even at high resolution on a spatial subset of the dark floor unit. The study also notes that there are some small-sized areas with low crater density at high resolution, suggesting possible local resurfacing processes by for example, wind (Warner et al., 2020).

A contribution on the general challenges with crater chronology reports the results of an independent assessment of the dark floor unit crater retention age using craters larger than 85 m, resulting in a retention age of 2 Gy, and

a conclusion that the dark floor unit is Amazonian, in agreement with previous studies (Rubanenko et al., 2021). The authors of this contribution did a spatial analysis of the distribution of the craters on the dark floor unit and highlighted some variability. The analysis excluded the presence of secondary crater clusters, which we know strongly affect the robustness of the results. The authors did, however, highlight low crater density areas close to the main delta fan (Rubanenko et al., 2021), which the authors interpreted as areas that were either recently exhumed or parts covered by wind-related deposits as previously suggested by Warner et al. (2020).

Therefore, several independent studies strongly argue for an Amazonian unit. Such a potential Amazonian sample would be of great value for the purpose of calibrating the Martian cratering chronology. The Martian crater chronology has been derived from the one established on the moon thanks to the link between observed lunar crater distribution and radioisotopic age of Apollo and Luna samples, taking into account the proximity of Mars to the main asteroid belt and the different gravity fields (Hartmann & Neukum, 2001; Ivanov, 2001). Alternative approaches exploit the collisional evolution model of the solar system to predict the impact rate and the size frequency distribution of craters through time (Marchi, 2021), also calibrated using the temporal constraints of the lunar samples. As the surface of the moon is largely older than 3.5 Ga, the lunar cratering chronology has been determined mainly from lunar samples older than 3.5 Ga (Stöffler & Ryder, 2001). Broadly, the lunar cratering chronology and consequently the Martian one remain poorly constrained for ages younger than 3.5 Ga (e.g., Hartmann & Neukum, 2001; Werner, 2019), so an Amazonian sample would help constrain cratering rates in this epoch.

The crater retention of the main delta of Jezero has been assessed in Mangold et al. (2020), who report a minimum model age of 3.5 Ga. The CSFD described in Mangold et al. has a slope lower than those of the isochrons, which suggests that the delta fan was emplaced before 3.5 Ga and has been continuously affected by resurfacing processes since then. Similar observations and conclusions are presented in Rubanenko et al. (2021). The presence of remnants around the main fan (Stack et al., 2020) and the exposure of inverted channel bars also argue for an intense erosion of the main delta fan since emplacement.

In summary, the slope of the crater size distribution of the crater population of the dark floor unit presented in several independent studies (Rubanenko et al., 2021; Shahrzad et al., 2019; Warner et al., 2020) is consistent with accumulation of craters with no significant modification except at small scale since about 2–2.5 Ga (range of crater based age model), while the deltaic deposit had a CSFD that has been interpreted to have a model crater retention age >3.5 Ga with subsequent erosion evidenced by the paucity of small craters.

3. Methodology

As highlighted in Section 2, we have a paradox between the apparent younger age of the dark floor unit compared to the delta units (Holm-Alwmark et al., 2021; Mangold et al., 2021) and the recent investigations placing the dark floor unit before the deltaic activity in the stratigraphy. In this study, we aim to evaluate this more comprehensively. We used three methods (morphological analysis from both in situ and orbital data analysis, crater density mapping, and impact crater formation modeling) to analyze the spatial variation of the crater density of the dark floor unit based on orbital data, and we modeled an impact crater accumulation scenario of a surface under gradual exhumation.

3.1. Orbital Data Analysis

We used an image mosaic basemap from the High Resolution Imaging Science Experiment (HiRISE) (McEwen et al., 2007) and derived digital terrain models (DTMs; 1 m/px). For context, we used Context Camera (CTX) image mosaic at 5 m/px from Dickson et al. (2018). The thickness measurements discussed in section 4b were made on HiRISE DTMs available on the Murray lab website (ESP_046060_1985_ESP_045994_1985 and ESP_023379_1985_ESP_023524_1985). The topographic profile displayed in Figure 5 and the topography displayed in Figure 4a are derived from a mosaic of CTX DTMs (Volat et al., 2022) produced by MarsSI application (Quantin-Nataf et al., 2018). For global Martian view, we used global MOLA data set (D. E. Smith et al., 2001) and Themis day-time mosaic (Edwards et al., 2011). All data were combined in a Geographic Information System (GIS) project.

3.2. Crater Density Map

We mapped all craters larger than 170 m (>200 craters) of the crater floor using the contour of the floor unit defined in Shahrzad et al. (2019). Below 170 m, as displayed in Figure 2, the density of crater of a theoretical

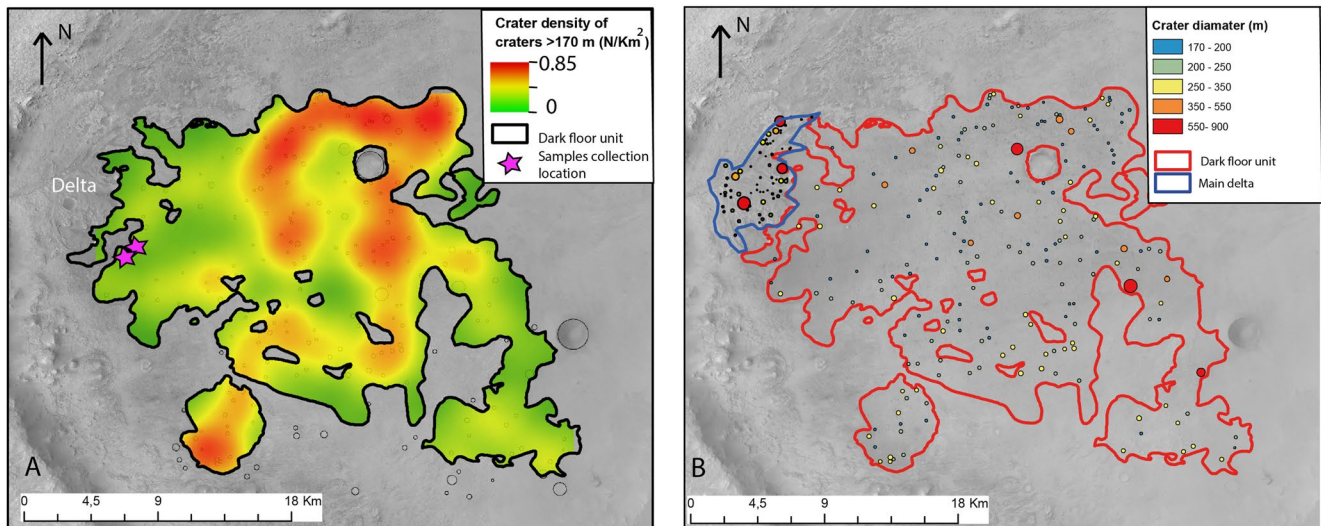


Figure 3. (a) Density of craters larger than 170 m of the dark crater floor unit of Jezero crater. The contour of the floor unit is from Shahrzad et al. (2019). The crater density is in N/km^2 . The pink stars denote the two locations of the 4 collected samples of the floor unit by Perseverance (Simon et al., 2023). (b) Map of the craters >170 m of both the main delta fan and the dark floor unit with a color code as a function of their size. We can qualitatively assess how the main delta fan is more impacted than the dark floor unit area at its foot.

~2.5 Gyr surface reaches the saturation line (Hartmann & Neukum, 2001). As Hartwell crater is within the contour of the floor unit, it was also included. All craters were then converted into a central point location from which we computed their spatial density using the ArcGIS software. We use a function which calculates a magnitude-per-unit area from points using a kernel function from Silverman (2018) to fit a smoothly tapered surface to each point. The resulting map is a raster where each cell ($100\text{ m} \times 100\text{ m}$) represents the crater density of craters larger than 170 m with units of craters per square kilometer (Figure 3). The dark floor unit thickness has been determined at 10 to 30 m (Schon et al., 2012; Shahrzad et al., 2019). It means that according to a crater depth/diameter of about 0.2, from 200 to 300 m in diameter (Rubanenko et al., 2021), the craters start to impact the underlying unit. Also, in the case of emplacement of the dark floor unit on a cratered paleo-surface, it means that the unit would not have completely buried craters larger than 200–300 m. In such a scenario, large craters may be older than the floor unit. A careful check of the morphology of large craters may thus be necessary to draw conclusions on their relative ages compared to dark floor unit emplacement. For instance, the observation of preserved ejecta blanket is an argument in favor of a pristine crater post-dating the crater floor unit emplacement. The lack of ejecta can however be explained by different scenarios.

3.3. In Situ Images

For the interpretation of sediment remnants, we include Mastcam-Z images. The Mastcam-Z instruments (Bell et al., 2021) are a suite of cameras mounted on the rover mast. The field of view ranges from $26 \times 19^\circ$ to $6 \times 5^\circ$ and the zoom system enables a spatial resolution of about 13.5 cm/pix at 2 km of distance (Bell et al., 2021). The motion of the mast enables imaging and large-format panoramas. Mastcam-Z has several multispectral modes including standard “human color” RGB filters (Bell et al., 2021). Figures 4c and 4d include extracts from the “Van-Zyl Overlook” panorama acquired on sol 63 and sol 132 as a mosaic of RGB color single images.

3.4. Impact Crater Modeling

Following the approach of the impact cratering model developed by Quantin-Nataf et al. (2019) to reproduce cratering with crater obliteration, we developed a model of impact cratering of a surface under exhumation due to the erosional retreat of a capping unit of a given thickness. The parameters of the model are the initial timing of the capping unit removal, the thickness of the capping unit, and the rate of horizontal retreat. The goal of this study is not to find a model that best fits the data but to use the model as a proof of concept to support working hypotheses.

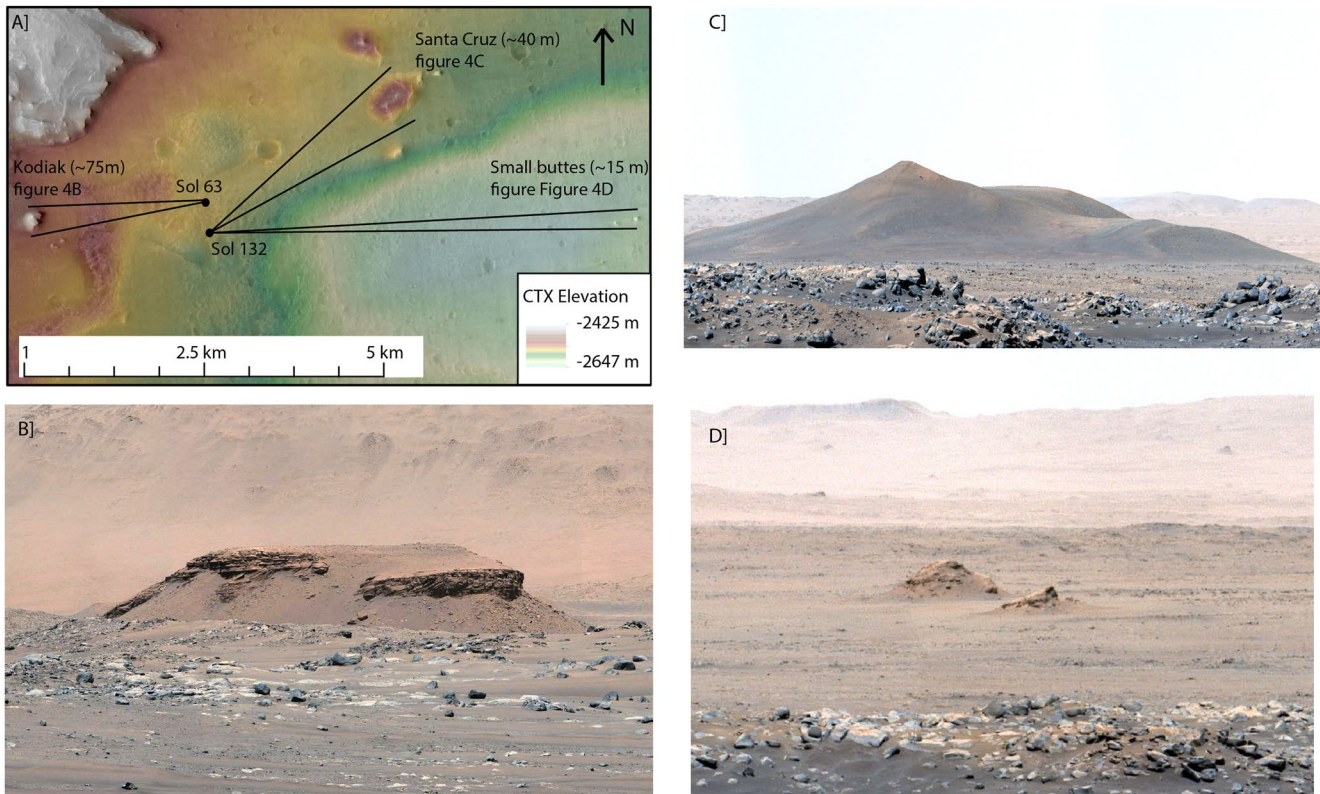


Figure 4. (a) CTX DTM overlay on CTX image mosaic. The dark line denotes the field of view corresponding to the ZCAM images displayed in the rest of the subfigures. (b) Part of the ZCAM mosaic of images taken on sol 63 at Van_Zyl Overlook location (Bell & Maki, 2021). The featured Kodiak butte in the scene is 300 m in width and about 2.3 km from the rover. (c) Part of ZCAM mosaic from images taken on sol 132 (Bell & Maki, 2021). The featured Santa Cruz butte in the scene is 600 m in width and about 3 km from the rover. (d) Part of ZCAM mosaic from images taken on sol 132 (Bell & Maki, 2021). The buttes in the scene are 60–80 m in width and about 6 km from the rover.

As a reminder, the basic equations of the model from Quantin-Nataf et al. (2019) are presented below. The assumptions behind the model as well as the test of the model are described in Quantin-Nataf et al. (2019). The model generates synthetic crater size distributions simulating impact crater production. The crater density of a planetary surface $n(D, T)$ is the number of craters per unit area (in km^2), where D (in km) is the crater diameter and T (in Ga) is the model age of the surface. This crater production function is assumed to have the same time dependence for all diameters (Hartmann, 2005; Hartmann & Neukum, 2001). Thus n is a function of two separated variables $n(D, T) = f(D)N(T)$. $N(T)$ is the accumulated number of craters larger than 1 km per unit area and is defined as follows (Neukum et al., 2001):

$$N_{D>1\text{km}}(T) = 5.44 \times 10^{-14} (e^{6.93T} - 1) + 8.38 \times 10^{-14} T \quad (1)$$

N' , the derivative of N , is the impact rate:

$$N'_{D>1\text{km}}(T) = \frac{dN_{D>1\text{km}}}{dT}(T) = 3.77 \times 10^{-13} e^{6.93T} + 8.38 \times 10 \quad (2)$$

The time evolution of the crater density is modeled according to the following equation:

$$\partial_T n(D, T) = f(D)N'(T) \quad (3)$$

The crater size distribution $f(D)$ is calculated by dividing a Martian isochron at time T from (Table 2 in Hartmann (2005)) by $N(T)$. The initial condition is $n(D, T = 0) = 0$. This equation is then integrated between T and $T + \Delta T$:

$$N(D, T + \Delta T) = n(D, T) + f(D)[N(T + \Delta T) - N(T)] \quad (4)$$

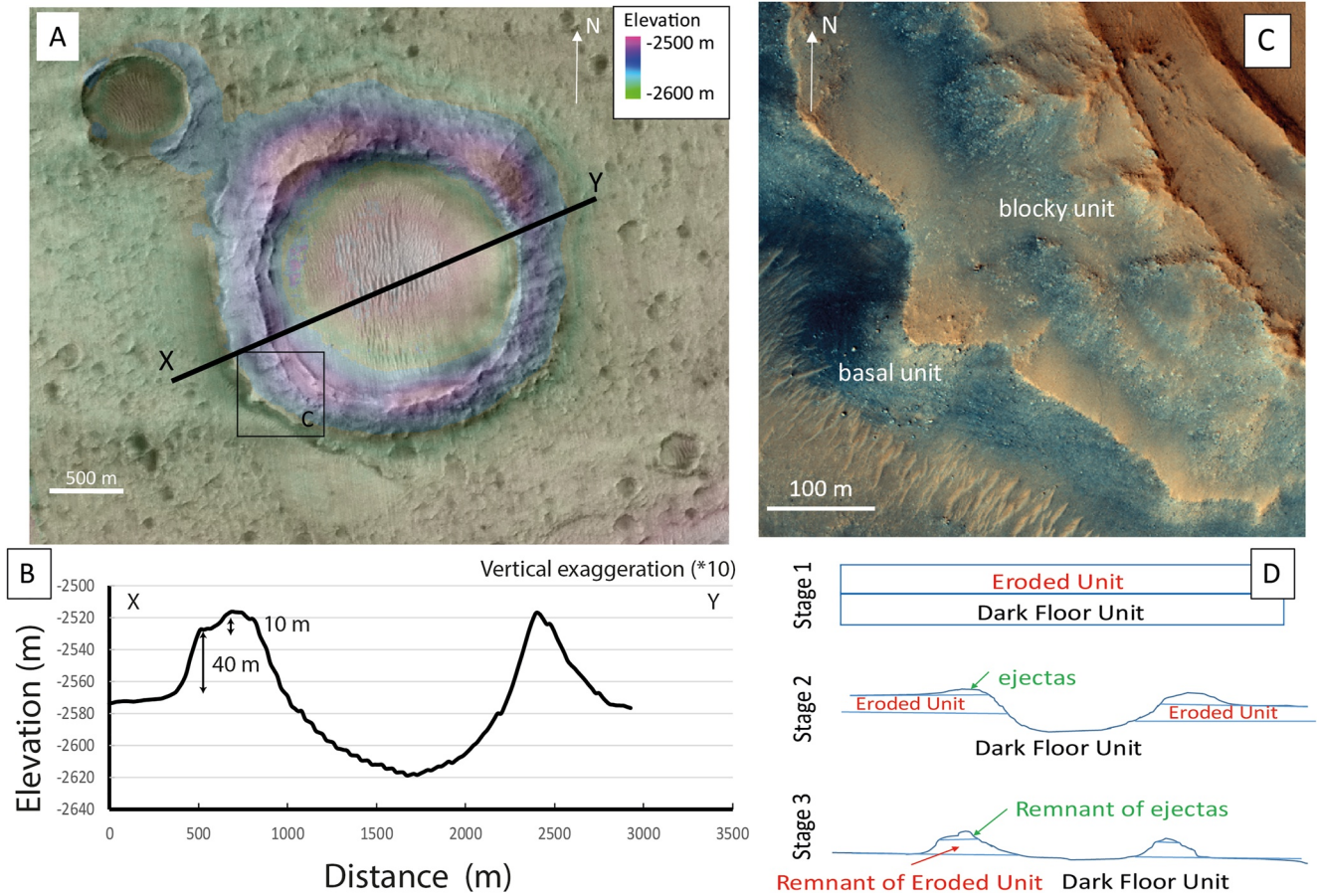


Figure 5. Hartwell crater. (a) Hirise Image and Elevation map from CTX DTM. The dark box is the enlargement of subfigure C. The XY topographic profile displayed in B is represented by the dark line. The shape of the ejecta of Hartwell crater is unusually small; the width of an ejecta blanket of a pristine crater is about 1 crater diameter wide. It appears that most of the ejecta of Hartwell crater has been eroded away. (b) Topographic profile XY from CTX DTM. (c) High Resolution Imaging Science Experiment color image zooming on the contact between the Jezero crater dark floor unit and Hartwell crater ejecta. (d) Schematic view of the succession of events leading to the unusual morphology of the remnant ejecta of Hartwell crater.

where $f(D)[N(T + \Delta T) - N(T)]$ is the number of craters added during the time step ΔT .

4. Orbital Data and In Situ Analysis

4.1. Crater Density Map

Our results show that the dark floor unit of Jezero has an unusual inhomogeneous crater density (Figure 3). The density of craters larger than 170 m is close to zero at the foot of the present-day delta, while it is as large as 0.85 craters/km² in the northeastern parts of the floor unit. The near lack of observed craters nearest to the delta, and in the area 7–8 km east of it, suggests a reduced exposure to bombardment compared to other regions. In contrast, the sections of the floor unit to the northeast and south have a crater density that corresponds to a model surface retention greater than 3 Ga, according to the age model from Hartmann (2005). As detailed in previous studies, no evidence of secondary crater clusters has been observed in the dark floor unit (Rubanenko et al., 2021).

Elsewhere on Mars, studies have pointed out the possible natural variability of crater density at small scale of small surfaces (Warner et al., 2015). For instance, Warner et al. (2015) reported crater densities at small scale ranging from 0 to 0.4 craters/km² on Amazonian surfaces. It may be an explanation for the floor of Jezero, and it would be a coincidence to have a lack of craters close to the main delta fan.

Another hypothesis to explain the inhomogeneous crater density is that it may be related to different subunits within the dark floor unit. Such a scenario would imply a period of formation/emplacement as old as >3 Gy for

the eastern part of the dark floor unit and a formation very recently for the parts of the unit that are close to the delta. No inner geological boundaries are observed to confirm this hypothesis from orbit. On the contrary, several independent studies (orbital data-based) of the dark floor unit (Goudge et al., 2012; Rubanenko et al., 2021; Shahrzad et al., 2019) have mapped this unit as a single unit with a very well defined external boundary.

A third hypothesis is related to the unit thickness. If there is significant variability in the thickness of the dark floor unit over the Jezero crater floor, then that could lead to variations in apparent crater retention ages over the unit. The variability would then be explained by the inhomogeneous burying of a cratered paleosurface by a layer of variable thickness. This hypothesis would imply a cratered paleo-surface below the dark floor unit and evidence of large variability in the thickness of the dark floor unit. Shahrzad et al. measured the thickness of the dark floor unit in more than 400 locations and conclude that it has a relatively homogeneous thickness of $13 \text{ m} \pm 0.8 \text{ m}$ (Shahrzad et al., 2019). There is no thickness variation correlated to the crater density variation observed here.

Without orbital evidence of subunits within the dark floor unit and without the identification of thickness variations in the unit, these results suggest that the floor unit, as a single unit (timely speaking), has experienced differential exposure to bombardment over the last 3 Ga. It seems inconceivable that a geologic unit could be emplaced systematically over the past 3 Ga, especially as its volcanic origin (Alwmark et al., 2023; B. Horgan et al., 2022) suggests a geologically short emplacement, when all adjacent units point toward a long lasting erosional environment (Mangold et al., 2021; Stack et al., 2020). We offer a more plausible hypothesis that the floor unit was buried and subsequently exhumed both gradually and unevenly away from the crater center. This hypothesis also explains why the crater size distribution is following the theoretical bombardment slope. In the next section, we review evidence in agreement with this hypothesis of burial and exhumation of the floor of Jezero crater.

4.2. Evidence for Erosion and Remnant Sedimentary Deposits

Several buttes have been described within Jezero crater in previous studies that have been interpreted as possible remnants of sedimentary deposits (e.g., Stack et al., 2020). The first butte studied in detail by Perseverance using in situ data was Kodiak (Figure 4b), which has been identified thanks to the Mars2020 payload as a well-conserved butte of deltaic deposits with well-identified topset, foreset and bottom-set layers. In Figure 4b, the upper cliff of the butte exposes layers interpreted as topsets (Mangold et al., 2021). The maximum thickness of the Kodiak butte is of the order of 70 m. Between Kodiak and the main delta body is an exposure of the flat lying dark floor unit (Figure 1), suggesting that a large pile of sediment has been eroded away between Kodiak and the main deltaic body, revealing the dark floor unit (Mangold et al., 2021). This strong erosion of the delta front through horizontal retreat can explain the very low crater density in this part of Jezero, immediately south and east of the actual delta front (Figure 3), evidence in favor of the exhumation of crater floor units older than the delta deposits.

The buttes eastward to the main delta named “channels islands” (Figure 1), including the highest hill called Santa Cruz, have been proposed to be either delta remnants or other types of sediment remnants from periods predating the actual fan (e.g., Stack et al., 2020). These buttes lie on the top of the dark floor unit according to a study dedicated to stratigraphic relationship between these buttes and the dark floor unit (Holm-Alwmark et al., 2021). This conclusion is based on a careful analysis of the topographic profiles of the contacts between the dark floor unit and the main delta fan and the surrounding buttes (Holm-Alwmark et al., 2021). There are no marginal depressions (erosional moats) around the contact between the deltaic deposits and the dark floor unit, as would be expected if the dark floor unit post-dated and embedded the deltaic deposits. Both the main delta fan and the surrounding buttes post-date the dark floor unit (Holm-Alwmark et al., 2021). Consequently, the buttes surrounding the main Jezero delta fan are potential candidates for remnants of the delta deposits. As displayed in Figure 4c, Santa Cruz buttes are not similar to Kodiak. The slopes of the butte are gentler, the color is darker and texture appears smoother without any upper cliff. The exact nature of these buttes is thus hard to determine but they may correspond to deposits of another kind compared to Kodiak. For instance, softer lacustrine deposits are possible given that the maximum elevation of Santa Cruz ($-2,520 \text{ m}$) is below the lowest elevation of the paleo-lake ($-2,500 \text{ m}$) determined at Kodiak from the transition between topsets and bottomsets (Mangold et al., 2021). In any cases, the facts that these remnants postdate the crater floor and were larger in the past explain that the area exposing the dark floor unit between Santa Cruz and the main fluvio-deltaic body of Jezero is almost free of impact craters, suggesting a recent exhumation. The initial results of the Perseverance delta front campaign by

RIMFAX (the ground penetrating radar of Mars2020 mission) confirm that the main delta fan is lying of the top of the dark floor unit (referred as the Maaz unit) (Russell et al., 2023).

Further east to Perseverance landing site, so further away from the main delta fan, Mastcam-Z observed two small buttes (Figure 4d). They are 15 km away from Jezero paleo-lake entrance and 7 km away from the actual delta front. These buttes are of the order of 15 m in height, as estimated on HiRISE DTM. They both display rocky cliffs similar in shape and color to Kodiak butte, although these buttes were too far from the rover to enable a more detailed investigation. It reveals that potential sediments were deposited near the center of Jezero and were eroded away, leaving these small remnant buttes. They are observed in a topographic low of the crater floor unit (Figure 4a) and also in an area with a very low crater density (Figure 3). This location may have been once a sedimentary basin where the floor unit would have been covered by a thicker sedimentary deposit. It is one of the locations near the center of the Jezero crater with a low crater density similar as the crater density observed close to the main delta fan.

The largest crater of the dark floor unit, Hartwell crater, has a diameter (D) of 1.7 km (Figures 2 and 4). Hartwell was excluded from the crater counting effort of Shahrzad et al. (2019) as the morphology of the crater is unusual, and it lacks ejecta. According to the authors, the crater could predate the floor unit emplacement. However, when observed at high resolution, no stratigraphic relationship suggests that the crater pre-date the formation of the dark floor unit. Indeed, no contact with erosional moats between the dark floor unit and the rim of the crater is observed, although it would be expected in a scenario where the dark floor unit was emplaced after the formation and erosion of Hartwell crater. The crater has rather an unusual pedestal shape. A topographic profile derived from the HiRISE-DTM (Figure 5b) and the color images (Figure 5c) reveal that the crater rim is composed of two distinct layers: The basal layer is about 40 m thick, smoothly eroded, while a second upper layer is blocky, as is expected for a proximal ejecta blanket (Figure 5c). The width of the ejecta blanket (Figure 5) is abnormally small for a crater of this size, suggesting that this crater is not in its pristine shape, as pointed out by Shahrzad et al. (2019). We expect the ejecta of a pristine crater to be of the order of 1 crater diameter wide (Collins et al., 2012). The width of the ejecta blanket of Hartwell crater should be in the order of 2 km while it is only a few hundreds of meters wide (Figure 5). It appears that most of the ejecta of Hartwell crater has been eroded away. The depth of the crater is about 100 m, which means that the crater has a depth to diameter ratio of the order of 0.06, which is significantly lower than expected for a pristine impact crater. This impact crater has thus been eroded. In the case of a scenario where Hartwell crater predates the emplacement of the dark floor unit, as interpreted by Shahrzad et al. (2019), it would imply that Hartwell crater was already eroded at the time of the dark floor unit emplacement. It would also suggest that the dark floor unit emplaced on an impacted and then eroded paleosurface. If that was the case, as the dark floor unit is only 10 s of meters thick, we should observe other embedded older eroded craters; however, this is not the case. We suggest an alternative hypothesis supported by observations of the occurrence of distinct layers visible in the remnants of the ejecta blanket: that the Hartwell crater was originally emplaced on a 40 m thick smooth unit that once overlaid the now-exposed dark floor unit. The scenario corresponding to this interpretation is presented in Figure 5d. The basal unit is now completely eroded in the vicinity of the crater, except in the outcrops just underneath the remnant ejecta blanket from this large crater, suggesting the ejecta blanket locally armored the capping unit against erosion creating the pedestal shape of the crater.

As in Gale crater (Banham et al., 2018), we also expect that the wind erosion played a strong role in the erosion and reworking of all weak material. Wind may have reworked the fluvio-lacustrine deposits into Aeolian sediments, eroded in turn during the Amazonian. Aeolian processes may also explain the asymmetry in impact density around Hartwell crater. Indeed, given that the E to W main wind direction seems predominant over time (Day & Dorn, 2019), the western side of Hartwell crater would be in the lee of wind, a situation leading to slower erosion of deposits than on the east side. The shape of small craters of the dark floor unit observed on HiRISE images (not discussed in this paper) is characterized by wind-related modification as suggested by Warner et al. (2020).

To summarize, there are several pieces of evidence suggesting that the dark crater floor unit was covered by other deposits leading to remnants in different places of Jezero crater close as well as far away from the main delta fan. Close to the main delta fan, we propose an extension of the main delta fan deposits, as it has been proposed for Kodiak buttes (Mangold et al., 2021), explaining the scarcity of small impact craters in this region after their erosion. Eastward of the Santa Cruz buttes, in the central part of Jezero may still have been deposited either lacustrine sediments or alluvial fills from periods devoid of lakes, before or after Jezero lake activity. The

thickness of such sediments is difficult to evaluate but deposits that are more distal should be thinner than the main deltaic deposit.

We propose the following sequence of events: (a) the formation of the dark floor unit, (b) its burial below sedimentary deposits of different kinds according to the location in Jezero, (c) the emplacement of Hartwell crater and (d) long-lived erosion and modification by Aeolian processes leading to current landscapes. In this scenario, Hartwell crater belongs to the population of craters that post-date the dark floor unit, contrary to the interpretation made by Shahrzad et al. (2019).

5. Modeling

Here, we used the equations presented in Section 3 to reproduce impact cratering on a 400 km² surface composed of two layers over >3 Ga. The basal layer is crater retaining and mimics the dark floor unit of Jezero. As soon as this unit is exposed to the impact bombardment, the craters accumulate without any subsequent modification. We assume an upper unit with a thickness of 40 m (the measured order of magnitude of maximum thickness of the Santa Cruz sedimentary remnant), which is under recessive erosion, and gradually exposes the subjacent basal layer. Such a scenario simulates a dark floor unit rapidly buried below a 40 m thick unit of about the same extent, which is deflating through time by lateral erosional retreat. While the upper unit is capping the subjacent resistant layer, only craters large enough to penetrate through the 40 m thick upper unit affect the subjacent layer. If we use the depth to diameter ratio of 0.2, craters larger than 800 m start to affect the underlying unit. Then, gradually, due to the lateral retreat of the upper unit, the basal unit is exposed to the bombardment and starts to retain craters of all sizes. The first exposed area of the basal unit would have a crater density corresponding to the beginning of the retreat of the upper unit, while the last exposed area would be crater free. The model assumes that the dark floor unit is made of a single unit with homogeneous crater retention properties and that the erosion rates are constant with time. The model also neglects the possible effects induced by target properties on the size of a crater produced by an impactor of a given size.

We ran several simulations with the exhumation starting age as a free parameter. The model using an exhumation starting at 3.2 Ga and a constant lateral retreat rate of 400 km²/3.2 Ga reproduces the observed crater distribution of the dark floor unit reported by Shahrzad et al. (2019), Warner et al. (2020) with craters smaller than D 700 m following the ~2.5 Ga model isochrons and craters larger than D 700 m with higher density (Figure 6). The largest craters penetrate the underlying dark floor unit and are not aligned with the size distribution of smaller craters. The apparent crater retention age of the floor of about 2.5 Ga derived from craters smaller than 700 m corresponds to an average exhumation age between the first parts of the floor that were exposed >3 Ga ago and others that were only recently exhumed. According to the crater density map presented in Figure 3, the exhumation started in northeast and southwest Jezero with the erosional front moving toward the western delta. A broad scenario of lateral Aeolian erosion from east to west would be in agreement with the dominant wind direction deduced from wind-related morphologies in Jezero crater (Day & Dorn, 2019). The undifferentiated smooth unit (Us, from Stack et al. (2020)) that covers the dark floor unit may represent a regolith-derived continued retreat of the western delta front or the last residual outcrop of the capping unit.

6. Discussion

The exhumation scenario of the dark floor unit (Figure 7) presented above explains the contradictory observations presented above. The dark floor unit would have been emplaced on the floor of Jezero crater before the deltaic activity >3.5 Ga. The deltaic/lacustrine activity dated at more than 3.5 Ga would have produced sediments burying the dark floor unit. Then, reworking of these sediments by Aeolian processes may have redistributed the sediments in Jezero crater, continuing the burying of the dark floor unit. Both in Santa Cruz hills and below the ejecta of Hartwell crater, the thickness of the deposits has been measured around 40 m attesting that deposits of the order of 40 m thickness were once present in Jezero crater, on top of the dark crater floor unit. Due to the presence of this 40-m thick sedimentary unit, the impact craters have to penetrate deeper than 40 m to leave a signature within the buried dark floor unit, and even more to reach the base of the dark floor unit, which is about 20 m thick (Shahrzad et al., 2019). As a result, only the statistics of impact craters larger than ~800 m may have recorded the entire span of time since the emplacement of the dark floor unit without being affected by the burying/exhumation history. Their statistics are very poorly constrained but would imply an age older than 3 Gy

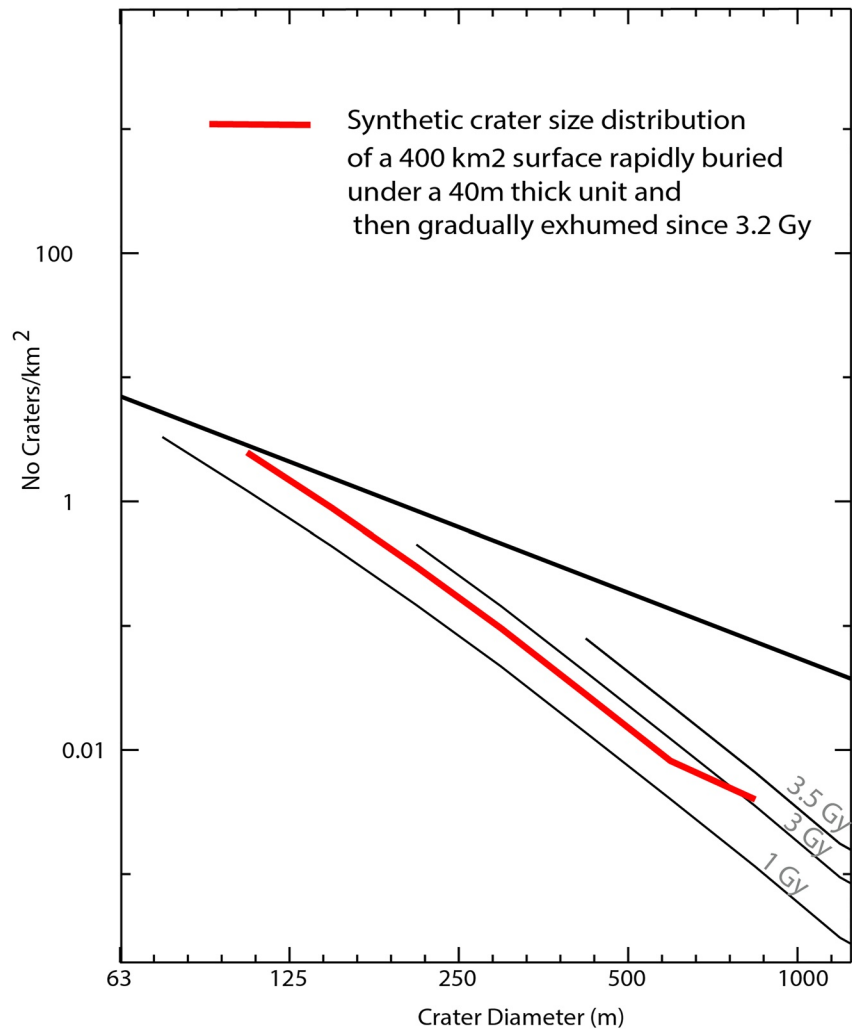


Figure 6. Synthetic crater size distribution of a 400 km² surface rapidly buried under a 40 m thick unit and then gradually exposed to bombardment since 3.2 Ga, using the crater production function of Hartmann (2005) and the time dependency from Neukum et al. (2001).

according to Figure 2. Then, due to the erosion of deltaic/lacustrine sediments, the dark floor unit would have been gradually exposed to bombardment, and would have accumulated craters smaller than 800 m, whose statistics are thus related to the exhumation age, rather than the timing of the crater floor emplacement. The thickness of the sediment has probably been variable in space and time, so the estimation of 40 m is an order of magnitude. The surface of the dark floor unit is not a flat surface either. It has a general west facing slope (Holm-Alwmark et al., 2021) and shows several depressions similar to the one where we observe remnant small buttes (Figure 4d). We may expect thicker sedimentary accumulation within local topographic lows. Then, under constant erosion, the thicker sedimentary sequences would last longer and protect the dark floor unit from bombardment during extended periods of time. It may explain the irregular crater density map beyond the east/west gradient observed in Figure 3.

The CSFD analysis at high resolution done in Warner et al. (2020) in the center of Jezero (Figure 2) attests that this part of the floor unit has been exposed since about 2.5 Ga. This means that the exhumation of the floor unit from the extreme eastern part of the crater to the center of the crater took at least 1 Ga (from about 3.5 to about 2.5 Ga). Then, it took the remaining 2.5 Ga of lateral erosion to exhume the floor unit up to the foot of the current delta front where the floor unit is almost crater free. As shown in this paper, a few sediment remnants, such as the Kodiak butte (Mangold et al., 2021) or the Channel Island buttes (Stack et al., 2020), are observed in Jezero crater (Figure 1), with a maximum height of 40 m above the modern floor, supporting the hypothesis

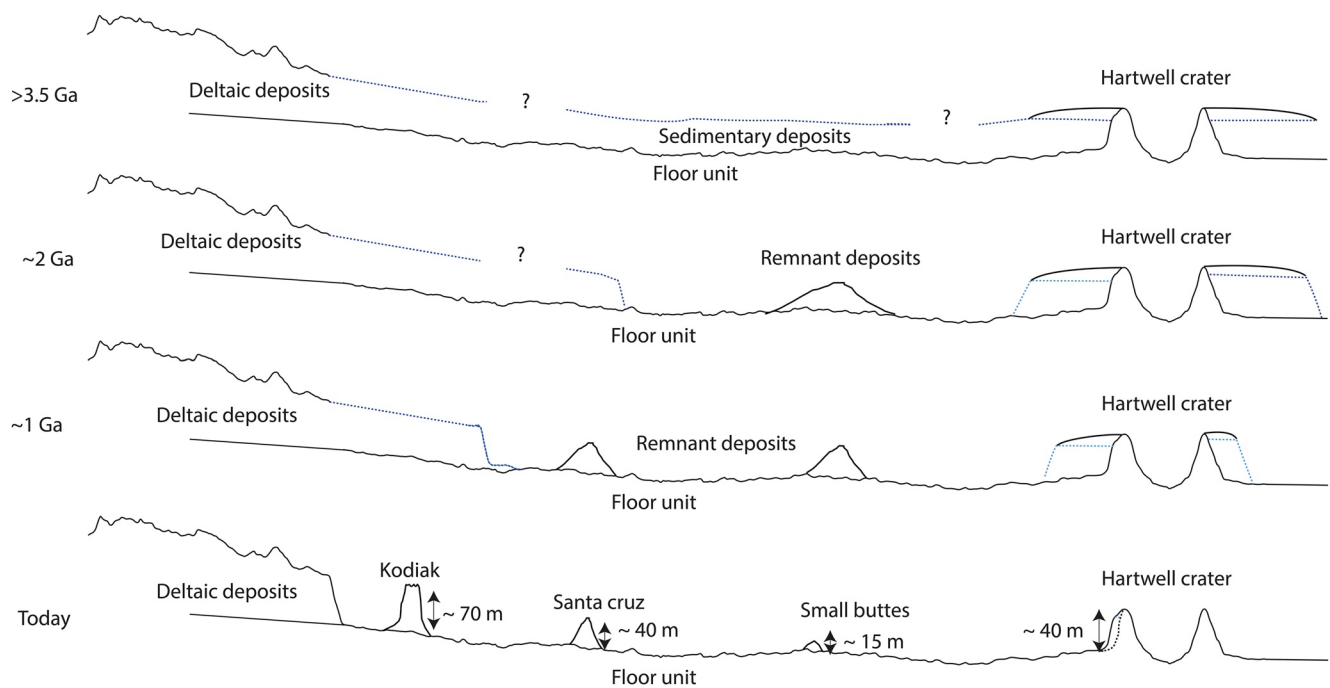


Figure 7. Schematic figure of the following exhumation scenario hypothesis: At >3.5 Gy, the dark floor unit would have been emplaced already but covered by a soft 40 m thick sedimentary unit. At 2 Gy the sedimentary deposit would have started to erode leaving some remnants and exposing about ½ of the dark floor unit to the meteoritic bombardment. At 1 Gy, the sedimentary unit would be further eroded, leaving more remnant deposits and exposing more surface of the dark floor unit to bombardment. Today, the sedimentary unit would be observed only in few remnant buttes and in the deltaic deposits.

of a more extensive sedimentary unit capping the dark floor unit in the past. The in situ analysis of Kodiak butte (Mangold et al., 2021) confirms that the butte is a remnant of deltaic deposits, implying that the deltaic deposits have been intensely eroded with horizontal retreat. Eroding a 40 m thick unit composed of soft material in more than 3 billion years implies a minimum erosion rate of 10^{-2} m/My. This value is in agreement with Amazonian erosion rates studied elsewhere on Mars in situ or by orbital analysis (Breton et al., 2022; Golombek et al., 2006; Quantin-Nataf et al., 2019). Within Jezero, the erosion rate of dark floor unit has been assessed at 10^{-3} to 10^{-4} m/Myr (Warner et al., 2020). This supports the hypothesis that the dark floor unit is resistant to erosion and consequently is a crater retaining unit. We also note that 10^{-2} m/My for the now retreated sedimentary unit is at the higher end of estimated values of Amazonian erosion rates, as well as other sedimentary units on Mars interpreted to be less resistant to erosion like the sediments of Meridiani Planum (Golombek et al., 2014).

Our interpretation of the observations implies that the dark floor unit is a homogeneous unit resistant to erosion with similar crater retention properties over the entire unit. The results presented in this paper suggest that this statement is robust at global scale, that is to say looking at the statistics of craters larger than 170 m. At this scale, there is no obliteration of craters over the entire unit as their size distribution is following the isochron slopes (Figure 2). However, the in situ investigation of the dark floor unit (Alwmark et al., 2023; B. Horgan et al., 2022; Sun et al., 2022) revealed that the Máaz formation is layered and comprised of five different members, with different properties that could influence erosion and crater retention. The primary spatial extension of these sub-units is not known even if some margin of potential lava flow may have been identified (Alwmark et al., 2023; B. Horgan et al., 2022). It may complicate the history we are presenting here: once exposed to bombardment, these different subunits may have eroded at different rates. Only a mapping of the <170 m crater density of the entire unit may decipher this potential additional complexity. This future work may be necessary to understand the exhumation ages of the different subunits at the local scale and their possible link with future measurement of exposure time to cosmic ray bombardment of the samples collected in the dark floor unit. Several Maaz samples were collected in part because they were high and “ideal” for cosmic ray exposure studies (Simon et al., 2023).

We have not yet addressed the outstanding issue of the emplacement age of the crater floor unit, which is critical for placing returned samples in context. To assess the crater based-model age of this floor unit, we can use the population of the craters larger than 500 m: even with a burial of the floor unit below 40 m of sediments, such

craters would reach the subjacent floor unit as Hartwell crater did. Nevertheless, the number of comparably large craters is too small to have a well-constrained age. We can only estimate a minimum model age of 3 Ga, in line with the original age estimate from Goudge et al. (2012) (Figure 2). We can also use the more densely impacted part of the floor unit such as the north east part (Figure 3) to assess the beginning of the exhumation history as a minimum age of the formation of the dark floor unit. The density of craters >170 m of the northeastern part of the floor unit also corresponds to a minimum model age of 3 Ga. According to several authors (Hundal et al., 2022; Sun & Stack, 2020), the dark floor unit within Jezero crater may be part of a larger unit exposed in the entire region of Nili Fossae. If so, to assess the age of this mega unit, we may propose for future work to track the spatially extended exposure of the dark unit outside Jezero to obtain robust statistics on the accumulation of craters larger than 500 m since the formation of the unit. The olivine-rich unit stratigraphically below the dark floor unit in Jezero has been dated at 3.8 Ga (Mandon et al., 2020). If we use the more dense part of the dark floor unit within Jezero as the beginning of the exhumation, it means that the dark floor unit emplaced between 3.8 Ga and >3 Gy.

Our scenario further has consequences for Mars sample return. One of the goals of sampling the dark floor unit was to calibrate the Martian cratering chronology. For this purpose, a sample has to be linked to well constrained statistics of craters accumulated since the formation of the unit. This is clearly not the case for Jezero crater, as (a) the craters <500 m have not recorded the time since the formation of the unit but rather the time since its exhumation, and (b) the statistics of craters >500 m are not well constrained because of the small size of the dark floor unit. To have robust statistics of craters larger than 500 m, like more than 100 craters, the area of a unit older than 3 Gy has to be larger than 10,000 km². However, we have to keep in mind that even on the Moon, where the cratering chronology has been established thanks to returned samples, many links between samples and crater counted areas were not ideal either (e.g., Stöffler & Ryder, 2001) and several minimum crater densities or poorly constrained crater densities have been used to build the cratering chronology curve (Neukum et al., 2001). Similarly, on Mars, we could use the density of craters of the more densely impacted part of the dark floor unit of Jezero (i.e., the northeastern region, Figure 3) as a minimum crater density to be linked to the formation age of the unit derived from the returned samples.

The burial history of the organic matter preservation is an advantage for preservation. We can assume that below 40 m of sediments, the floor unit has been protected from cosmic ray bombardment and the resulting potential degradation of organic matter degradation (Farley et al., 2013). The part of the floor unit closer to the delta is therefore the most promising location for sampling. The floor unit sample locations, as part of the crater floor campaign (Sun et al., 2022), are not exactly at the base of the delta but are in the part of the floor unit that was most recently exhumed according to Figure 3.

7. Conclusion

While other studies have suggested that the dark floor unit in Jezero crater has an apparently young age, overlying and onlapping all other emplaced units, we present results here which are consistent with the floor unit predating the delta and implying that both the delta and floor are >3 Gy. Several contradictory observations about the emplacement history of the dark floor unit can be resolved if it is assumed to be resistant to erosion, initially buried below a few tens of meters thick unit that gradually eroded away due to Aeolian processes from the northeast to the west, resulting in uneven exposure to impact bombardment over 3 Ga. In this scenario, we show that the floor unit regions with highest crater density are the most important for estimating a minimum floor unit emplacement age. This scenario also has consequences for Mars sample return. Due to the complexity of its exposure history, the Jezero dark crater floor unit will require additional detailed analysis to understand how its samples can be used to inform the Martian cratering chronology. Our current investigation can only constrain the emplacement of the dark floor unit between the following crater-based model ages: >3 and 3.8 Gy.

Data Availability Statement

The orbital data used in this manuscript are available at this facility (note that users have to be registered or to create an account): marssi.univ-lyon1.fr. The crater statistics files used in this paper are from previous publications (Goudge et al., 2012; Shahrzad et al., 2019; Warner et al., 2020). Data from Warner et al. (2020) are recorded under this DOI <https://doi.org/10.6084/m9.figshare.12582833>. The Mast-cam images are available on the Planetary Data System (PDS) (Bell et al., 2021).

Acknowledgments

CQN, ED, JL, LM, NM are supported by the French space agency (CNES). SA acknowledges financial support from the Swedish Research Council (Grant 2017-06388). KK was supported by the Carlsberg foundation Grant CF19-0023. BH is funded by NASA's Mars 2020 Project via a subcontract from the California Institute of Technology/Jet Propulsion Laboratory to Arizona State University (subcontract 1511125). JS, BC, and DS are supported by the Mars 2020 Returned Sample Science Participating Scientist Program. SW was supported by BMWK. We thank the reviewers, especially Nicholas Warner for his comments, which greatly helped to improve the manuscript.

References

- Alwmark, S., Horgan, B., Udry, A., Bechtold, A., Fagents, S., Ravanis, E., et al. (2023). Diverse lava flow morphologies in the stratigraphy of the Jezero crater floor. *Journal of Geophysical Research: Planets*, *128*, e2022JE007446. <https://doi.org/10.1029/2022je007446>
- Banham, S. G., Gupta, S., Rubin, D. M., Watkins, J. A., Sumner, D. Y., Edgett, K. S., et al. (2018). Ancient Martian Aeolian processes and palaeomorphology reconstructed from the Stimson formation on the lower slope of Aeolis Mons, Gale crater, Mars. *Sedimentology*, *65*(4), 993–1042. <https://doi.org/10.1111/sed.12469>
- Beaty, D. W., Grady, M. M., McSween, H. Y., Sefton-Nash, E., Carrier, B. L., Altieri, F., et al. (2019). The potential science and engineering value of samples delivered to Earth by Mars sample return. *Meteoritics & Planetary Science*, *54*, 667–671. <https://doi.org/10.1111/maps.13242>
- Bell, J. F., & Maki, J. N. (2021). Mars 2020 mast camera zoom Bundle, from Arizona state University Mastcam-Z instrument team, calibrated products. *NASA Planetary Data System*. <https://doi.org/10.17189/Q3TS-C749>
- Bell, J. F., Maki, J. N., Mehali, G. L., Ravine, M. A., Caplinger, M. A., Bailey, Z. J., et al. (2021). The Mars 2020 Perseverance rover mast camera zoom (Mastcam-Z) multispectral, Stereoscopic imaging investigation. *Space Science Reviews*, *217*(1), 24. <https://doi.org/10.1007/s11214-020-00755-x>
- Breton, S., Quantin-Nataf, C., Pan, L., Mandon, L., & Volat, M. (2022). Insight into Martian crater degradation history based on crater depth and diameter statistics. *Icarus*, *377*, 114898. <https://doi.org/10.1016/j.icarus.2022.114898>
- Brown, A. J., Viviano, C. E., & Goudge, T. A. (2020). Olivine-carbonate mineralogy of the Jezero crater region. *Journal of Geophysical Research: Planets*, *125*(3), e2019JE006011. <https://doi.org/10.1029/2019JE006011>
- Collins, G. S., Melosh, H. J., & Osinski, G. R. (2012). The impact-cratering process. *Elements*, *8*(1), 25–30. <https://doi.org/10.2113/gselements.8.1.25>
- Day, M., & Dorn, T. (2019). Wind in Jezero Crater, Mars. *Geophysical Research Letters*, *46*(6), 3099–3107. <https://doi.org/10.1029/2019GL082218>
- Dickson, J. L., Kerber, L. A., Fassett, C. I., & Ehlmann, B. L. (2018). A global, blended CTX mosaic of Mars with vectorized seam mapping: A new mosaicking pipeline using principles of non-destructive image editing. In *49th Lunar and Planetary Science Conference*.
- Edwards, C. S., Nowicki, K. J., Christensen, P. R., Hill, J., Gorelick, N., & Murray, K. (2011). Mosaicking of global planetary image datasets: 1. Techniques and data processing for thermal emission imaging system (THEMIS) multi-spectral data. *Journal of Geophysical Research*, *116*(E10), E10008. <https://doi.org/10.1029/2010JE003755>
- Farley, K. A., Malespin, C., Mahaffy, P., & Grotzinger, J. P. (2013). In *Situ radiometric and exposure age dating of the Martian surface—Supplementary materials* (pp. 1–9). <https://doi.org/10.1126/science.1247166>
- Farley, K. A., Stack-Morgan, K. M., Shuster, D. L., Horgan, B. H. N., Hurowitz, J. A., Tarnas, J. D., et al. (2022). Aqueously altered igneous rocks sampled on the floor of Jezero crater, Mars. *Science*, *377*(6614). <https://doi.org/10.1126/science.abo2196>
- Golombek, M. P., Grant, J. A., Crumpler, L. S., Greeley, R., Arvidson, R. E., Bell, J. F., et al. (2006). Erosion rates at the Mars Exploration Rover landing sites and long-term climate change on Mars. *Journal of Geophysical Research: Planets*, *111*(12), 1–14. <https://doi.org/10.1029/2006JE002754>
- Golombek, M. P., Warner, N. H., Ganti, V., Lamb, M. P., Parker, T. J., Ferguson, R. L., & Sullivan, R. (2014). Small crater modification on Meridiani Planum and implications for erosion rates and climate change on Mars. *Journal of Geophysical Research: Planets*, *119*(12), 2522–2547. <https://doi.org/10.1002/2014JE004658>
- Goudge, T. A., Head, J. W., Mustard, J. F., & Fassett, C. I. (2012). An analysis of open-basin Lake deposits on Mars: Evidence for the nature of associated lacustrine deposits and post-lacustrine modification processes. *Icarus*, *219*(1), 211–229. <https://doi.org/10.1016/j.icarus.2012.02.027>
- Goudge, T. A., Mustard, J. F., Head, J. W., Fassett, C. I., & Wiseman, S. M. (2015). Assessing the mineralogy of the watershed and fan deposits of the Jezero crater Paleolake system, Mars. *Journal of Geophysical Research: Planets*, *120*(4), 775–808. <https://doi.org/10.1002/2014JE004782>
- Hartmann, W. K. (2005). Martian cratering 8: Isochron refinement and the chronology of Mars. *Icarus*, *174*(2), 294–320. <https://doi.org/10.1016/j.icarus.2004.11.023>
- Hartmann, W. K., & Neukum, G. (2001). Cratering chronology and the evolution of Mars. *Space Science Reviews*, *96*(1–4), 165–194. <https://doi.org/10.1023/A:1011945222010>
- Holm-Alwmark, S., Kinch, K. M., Hansen, M. D., Shahrzad, S., Svennevig, K., Abbey, W. J., et al. (2021). Stratigraphic relationships in Jezero Crater, Mars: Constraints on the timing of fluvial-lacustrine activity from orbital observations. *Journal of Geophysical Research: Planets*, *126*(7), e2021JE006840. <https://doi.org/10.1029/2021JE006840>
- Horgan, B., Udry, A., Rice, M., Alwmark, S., Amundsen, H., Bell, J., et al. (2022). Mineralogy, morphology, and emplacement history of the Maaz formation on the Jezero crater floor from orbital and rover observations. *ESS Open Archive*. <https://doi.org/10.1002/essoar.10512674.1>
- Horgan, B. H. N., Anderson, R. B., Dromart, G., Amador, E. S., & Rice, M. S. (2020). The mineral diversity of Jezero crater: Evidence for possible lacustrine carbonates on Mars. *Icarus*, *339*, 113526. <https://doi.org/10.1016/j.icarus.2019.113526>
- Hundal, C. B., Mustard, J. F., Kremer, C. H., Tarnas, J. D., & Pascuzzo, A. C. (2022). The Circum-Isidis capping unit: An extensive regional Ashfall deposit exposed in Jezero Crater. *Geophysical Research Letters*, *49*(9), e96920. <https://doi.org/10.1029/2021GL096920>
- Ivanov, B. A. (2001). Mars/Moon cratering rate ratio estimates. *Space Science Reviews*, *96*(1–4), 87–104. <https://doi.org/10.1023/A:1011941121102>
- Kite, E. S., & Mayer, D. P. (2017). Mars sedimentary rock erosion rates constrained using crater counts, with applications to organic-matter preservation and to the global dust cycle. *Icarus*, *286*, 212–222. <https://doi.org/10.1016/j.icarus.2016.10.010>
- Mandon, L., Quantin-Nataf, C., Royer, C., Beck, P., Fouchet, T., Johnson, J. R., et al. (2022). Reflectance of Jezero crater floor: 2. Mineralogical interpretation. *Journal of Geophysical Research*, *127*, e2022JE007450. <https://doi.org/10.1029/2022je007450>
- Mandon, L., Quantin-Nataf, C., Thollot, P., Mangold, N., Lozac'h, L., Dromart, G., et al. (2020). Refining the age, emplacement and alteration scenarios of the olivine-rich unit in the Nili Fossae region, Mars. *Icarus*, *336*, 113436. <https://doi.org/10.1016/j.icarus.2019.113436>
- Mangold, N., Dromart, G., Ansan, V., Salese, F., Kleinhans, M. G., Massé, M., et al. (2020). Fluvial regimes, Morphometry, and age of Jezero crater paleolake inlet Valleys and their exobiological significance for the 2020 rover mission landing site. *Astrobiology*, *20*(8), 994–1013. <https://doi.org/10.1089/ast.2019.2132>
- Mangold, N., Gupta, S., Gasnault, O., Dromart, G., Tarnas, J. D., Sholes, S. F., et al. (2021). Perseverance rover reveals an ancient delta-lake system and flood deposits at Jezero crater, Mars. *Science*, *374*(6568), 711–717. <https://doi.org/10.1126/science.abc4051>
- Marchi, S. (2021). A new Martian crater chronology: Implications for Jezero Crater. *The Astronomical Journal*, *161*(4), 187. <https://doi.org/10.3847/1538-3881/abe417>
- McEwen, A. S., Eliason, E. M., Bergstrom, J. W., Bridges, N. T., Hansen, C. J., Delamere, W. A., et al. (2007). Mars reconnaissance orbiter's high resolution imaging science experiment (HiRISE). *Journal of Geophysical Research: Planets*, *112*(5), 1–40. <https://doi.org/10.1029/2005JE002605>
- Michael, G. G. (2013). Planetary surface dating from crater size-frequency distribution measurements: Multiple resurfacing episodes and differential isochron fitting. *Icarus*, *226*(1), 885–890. <https://doi.org/10.1016/j.icarus.2013.07.004>

- Neukum, G., Ivanov, B. A., & Hartmann, W. K. (2001). Cratering records in the inner solar system in relation to the lunar reference system. *Space Science Reviews*, 96(1/4), 55–86. <https://doi.org/10.1023/A:1011989004263>
- Quantin-Nataf, C., Craddock, R. A., Dubuffet, F., Lozac'h, L., & Martinot, M. (2019). Decline of crater obliteration rates during early Martian history. *Icarus*, 317, 427–433. <https://doi.org/10.1016/j.icarus.2018.08.005>
- Quantin-Nataf, C., Lozac'h, L., Thollot, P., Loizeau, D., Bultel, B., Fernando, J., et al. (2018). MarsSI: Martian surface data processing information system. *Planetary and Space Science*, 150, 157–170. <https://doi.org/10.1016/j.pss.2017.09.014>
- Rubanenko, L., Powell, T., Williams, J.-P., Daubar, I., Edgett, K., & Paige, D. (2021). Challenges in crater chronology on Mars as reflected in Jezero crater (pp. 97–122). <https://doi.org/10.1016/B978-0-12-820245-6.00005-7>
- Russell, P. S., Paige, D. A., Hamran, S.-E., Amundsen, H., & Annex, A. (2023). Stratigraphy relationships of the delta and Crater Floor in Jezero Crater from RIMFAX GPR observations. In *Lunar and Planetary sciences conference*.
- Schon, S. C., Head, J. W., & Fassett, C. I. (2012). An overfilled lacustrine system and progradational delta in Jezero crater, Mars: Implications for Noachian climate. *Planetary and Space Science*, 67(1), 28–45. <https://doi.org/10.1016/j.pss.2012.02.003>
- Shahrazad, S., Kinch, K. M., Goudge, T. A., Fassett, C. I., Needham, D. H., Quantin-Nataf, C., & Knudsen, C. P. (2019). Crater statistics on the dark-toned, mafic floor unit in Jezero Crater, Mars. *Geophysical Research Letters*, 46(5), 2408–2416. <https://doi.org/10.1029/2018GL081402>
- Silverman, B. W. (2018). Density estimation: For statistics and data analysis. In *Density estimation: For statistics and data analysis*. <https://doi.org/10.1201/9781315140919>
- Simon, J. I., Hickman-Lewis, K., Cohen, B. A., Mayhew, L. E., Shuster, D. L., Debaille, V., et al. (2023). Samples collected from the floor of Jezero Crater with the Mars 2020 perseverance rover. *Journal of Geophysical Research: Planets*, 128, e2022JE007474. <https://doi.org/10.1029/2022je007474>
- Smith, D. E., Zuber, M. T., Frey, H. V., Garvin, J. B., Head, J. W., Muhleman, D. O., et al. (2001). Mars Orbiter Laser Altimeter: Experiment summary after the first year of global mapping of Mars. *Journal of Geophysical Research: Planets*, 106(E10), 23689–23722. <https://doi.org/10.1029/2000JE001364>
- Smith, M. D., Bandfield, J. L., Christensen, P. R., & Richardson, M. I. (2003). Thermal Emission Imaging System (THEMIS) infrared observations of atmospheric dust and water ice cloud optical depth. *Journal of Geophysical Research*, 108(E11), 5115. <https://doi.org/10.1029/2003JE002115>
- Stack, K. M., Williams, N. R., Calef, F., Sun, V. Z., Williford, K. H., Farley, K. A., et al. (2020). Photogeologic map of the Perseverance rover field site in Jezero crater constructed by the Mars 2020 science team. *Space Science Reviews*, 216(8), 127. <https://doi.org/10.1007/s11214-020-00739-x>
- Stöffler, D., & Ryder, G. (2001). Stratigraphy and isotope ages of lunar geologic units: Chronological standard for the inner solar system. *Space Science Reviews*, 96(1/4), 9–54. <https://doi.org/10.1023/A:1011937020193>
- Sun, V. Z., Hand, K. P., Stack, K. M., Farley, K. A., Simon, J. I., Newman, C., et al. (2023). Overview and results from the Mars 2020 Perseverance rover's first science campaign on the Jezero crater floor. *Journal of Geophysical Research: Planets*, 128, e2022JE007613. <https://doi.org/10.1029/2022JE007613>
- Sun, V. Z., & Stack, K. M. (2020). *Geologic map of Jezero crater and the Nili Planum region, Mars* (Vol. 3464). U.S. Geological Survey Scientific Investigations Map. pamphlet 1. <https://doi.org/10.3133/sim3464>
- Udry, A., Ostwald, A., Sautter, V., Cousin, A., Beyssac, O., Forni, O., et al. (2022). A Mars 2020 Perseverance SuperCam Perspective on the Igneous Nature of the Máaz formation at Jezero crater and link with Séítah, Mars. *Journal of Geophysical Research: Planets*, 127, e2022JE007440. <https://doi.org/10.1029/2022JE007440>
- Volat, M., Quantin-Nataf, C., & Dehecq, A. (2022). Digital elevation model workflow improvements for the MarsSI platform and resulting orthorectified mosaic of Oxia Planum, the landing site of the ExoMars 2022 rover. *Planetary and Space Science*, 222, 105552. <https://doi.org/10.1016/j.pss.2022.105552>
- Warner, N. H., Gupta, S., Calef, F., Grindrod, P., Boll, N., & Goddard, K. (2015). Minimum effective area for high resolution crater counting of Martian terrains. *Icarus*, 245, 198–240. <https://doi.org/10.1016/j.icarus.2014.09.024>
- Warner, N. H., Schuyler, A. J., Rogers, A. D., Golombek, M. P., Grant, J., Wilson, S., et al. (2020). Crater Morphometry on the mafic floor unit at Jezero Crater, Mars: Comparisons to a known Basaltic Lava plain at the InSight landing site. *Geophysical Research Letters*, 47(17), e89607. <https://doi.org/10.1029/2020GL089607>
- Werner, S. C. (2019). In situ calibration of the Martian cratering chronology. *Meteoritics & Planetary Sciences*, 54(5), 1182–1193. <https://doi.org/10.1111/maps.13263>
- Wiens, R., Udry, A., Beyssac, O., Quantin-Nataf, C., Mangold, N., Cousin, A., et al. (2022). Compositionally and density stratified igneous terrain in Jezero crater, Mars. *Science Advances*, 8(34). <https://doi.org/10.1126/sciadv.abo3399>